Three-Dimensional Electron Microscopy of Mesoporous Materials—Recent Strides Towards Spatial Imaging at the Nanometer Scale

Krijn P. de Jong*[a] and Abraham J. Koster[b]

KEYWORDS:

electron tomography · holography · materials science · mesoporous materials · TEM · three-dimensional imaging

Mesoporous materials are of particular interest to major application fields, such as in catalysis, separation and chemical sensing. Ordered mesoporous materials have been studied extensively over the last decade involving MCM[1] and SBA[2] as important representative classes. These materials contain ordered pores and cavities with sizes ranging typically from 3 – 10 nm, whereas the pore walls consist of amorphous materials such as silicon dioxide. Recent reviews on this dynamic field of materials science are available.[3–5] Disordered mesoporous materials, in contrast, display random pore systems (2 – 50 nm) and up until now are predominantly the materials of choice for the application fields indicated above. Examples of the latter materials are zeolite crystals that contain random mesopores next to intracrystalline micropores[6] and metal clusters supported on nanosized oxide particles.[7] In order to further exploit these mesoporous materials, their characterisation at the nanometer scale is of great importance, in particular the size, shape and connectivity of the mesopores. Macroscopic techniques to characterise the pores are available, such as physisorption, that provide us with averaged data with global models of pore shape.[8, 9] A microscopic extension of this characterisation is highly desirable.[10, 11] Significant advances toward this goal have been published recently. Three-dimensional electron microscopy (3D-TEM) techniques and results are at the basis of these advances and the subject of this Highlight.

[a] *K. P. de Jong*
Inorganic Chemistry and Catalysis
Debye Institute
P.O. Box 80083
3508 TB Utrecht (The Netherlands)
Fax: (+31) 30-2511-027
E-mail: k.p.dejong@chem.uu.nl

[b] *A. J. Koster*
Department of Molecular Cell Biology
Utrecht University
Padualaan 8
3584 CH Utrecht (The Netherlands)

Revealing Structural Detail in the Third Dimension with 3D Electron Microscopy

Transmission Electron Microscopy (TEM) is the only available technique to obtain direct structural information at nanometer scale resolution for porous materials. The importance of three-dimensional (3D) imaging with TEM becomes clear when we realize that the electron beam, imaging the sample, transverses *through* the sample. Thus a two-dimensional (2D) image is obtained of an inherently 3D sample. At a first approximation, the 2D image can be regarded as a 2D projection of the 3D sample under investigation. As a result, high-resolution (0.1 – 0.3 nm) interpretation of the 2D images will hardly be possible in spite of both the high-resolution capabilities of the TEM (0.1 – 0.3 nm) and the high-resolution information contained within the 3D sample (atom distribution). The difficulty is not only due to fundamental physical aspects of image formation related to electron – specimen interactions, but more so due to the fact that structural features within the 3D sample are projected—and overlap—into a 2D image. A case in point is a (2D) TEM image of MCM-41 that has been published many times with a representative example in Figure 1. The beautiful hexagonal ordering of the mesopores is apparent but essentially no information can be deduced on the structure of the pores perpendicular to the plane of projection. Consequently, the resolution in the third dimension is not better than the thickness of the sample. During the last five years a number of methods and techniques were developed to make it possible to retrieve structural information also in the third dimension at nanometer-scale resolution.

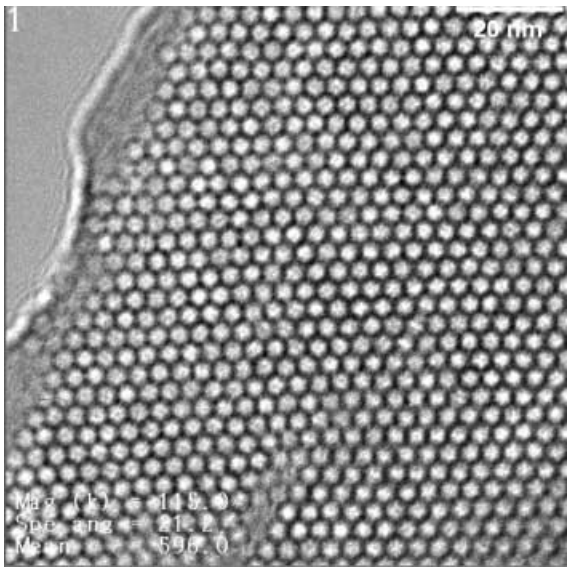

Figure 1. *TEM image of MCM-41 with a pore diameter of ~3 nm. Scale bar 20 nm.*

  1439-4235/02/03/09 $ 20.00+.50/0 CHEMPHYSCHEM **2002**, 3, 776 – 780

Through-Focus Series Reconstruction and Electron Holography

Before going into some detail on 3D imaging approaches, we point out that the relation between a recorded 2D image and the 3D sample under investigation depends highly on the properties of the 3D sample.[12] For example, in many cases for very thin samples ($< 2-50$ nm) *phase contrast* will be the most dominant type of image-contrast formation mechanism. For phase-contrast specimens, the 2D image contrast is related to phase changes experienced by the electron beam passing transverse through the specimen. For those specimens and under certain imaging conditions, a bright area within a 2D image can correspond to a (projected) 3D volume within the sample that is composed of a type of material that induces different phase changes to the electron beam compared to its surroundings. For thin samples, where weak phase-contrast imaging will be the most dominant type of image contrast, the recording of a through-focus series followed by a focal series reconstruction approach[13] can be effective in obtaining high-resolution 3D structural information of the material. Related to the through-focus series approach is electron holography,[14] which is also particularly suitable to acquire 3D information on small particles (weak-phase objects). As an application of holography to image metal nanoparticles on support material we refer to Datye et al.[15] His group made use of the phase image derived from an electron hologram to show unequivocally that the 8 nm Pd particles in Pd/SiO_2 (a model catalyst) have a facetted internal void of ~ 3 nm.

Electron Tomography

For thicker samples ($> 50-500$ nm), the most dominant type of 2D image contrast will, most likely, not be phase contrast but *scattering contrast*. In that case, a dark area within a 2D image will correspond to a (projected) 3D volume within the sample that contains material with a higher *mass density* compared to its surroundings. More specifically, the high mass density encountered by the electron beam causes a considerable number of the electrons to scatter outside the objective aperture. This will give rise to the relation that dark areas within the 2D images correspond to areas with a high mass density. For strongly diffracting specimens, neither phase contrast nor scattering contrast will be the most dominant type of image contrast formation. In that case, the brightness of a pixel in a recorded 2D image does not have a straightforward correspondence with either the (projected) mass or phase, but will be related to Bragg angle diffraction conditions.

In 3D-TEM, the approach in which a 3D image of an *individual piece of material* is reconstructed from typically *50–150 images* of the sample tilted at various angles (see Figure 2) is often referred to as electron tomography. With electron tomography, each individual image can be regarded as a 2D projection of some property of the sample (for example, mass) provided that phase contrast and/or scattering contrast are the dominant types of image formation mechanism. The ultimately attainable resolution of electron tomography will be limited by the resolution present within each of the individual 2D images. In most cases, a more practical limit to the resolution in the 3D image is set by the specimen tilt range and specimen tilt increments chosen to collect a tilt series (such as from -70° to $+70^\circ$ with 1° tilt intervals to give 141 images). An indication of the attainable resolution is given by the relationship $r = \pi d/n$, where r is the resolution, d is the sample thickness and n is the number of 2D images.[19] For instance, the 3D resolution of a 100 nm thick zeolite particle will be in the order of 2 nm when 141 images are recorded.

During the last decade within the life sciences, electron tomography[17–19] and its automation[20, 21] has developed rapidly. Presently, using automated data collection systems that enable direct recording of images (CCD camera), 141 images can be obtained within 20 minutes over a wide angular range ($\pm 70^\circ$). After data collection, the subsequent 3D reconstruction comprises data alignment and 3D reconstruction via back projection. For a description of the reconstruction approach, see Baumeister and Steven.[22] The reconstructed 3D images are volumes of data that can be presented in a variety of ways. The most straightforward approach is to consider the 3D reconstruction as a stack of thin (virtual) 2D slices (in our applications typically 2 nm thick) cut through the reconstructed structure (volume). Computer programs can display each of these virtual slices and it is possible to study details of the pore systems that would, in a conventional 2D-TEM image, have been otherwise obscured by overlapping material above and below the 2D slice. As an example we present recent results obtained by Koster et al.[16] and Janssen et al.[23] to image

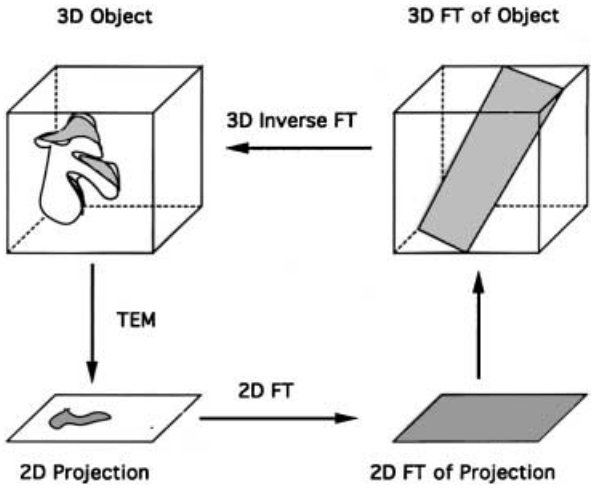

Figure 2. *Principle of 3D-TEM techniques. A series of 2D projections is used to allow Fourier transformation (FT) and back transformation to obtain a reconstruction of the 3D object. The 3D Fourier transform (right) of the 3D structure of interest (left) serves as a melting pot for combining electron microscopy data collected in either the electron crystallography or electron tomography approaches.*

mesopores in zeolite crystals. In Figure 3 we compare the results from conventional (2D-) TEM and 3D-TEM. The mesopores in this strongly dealuminated zeolite Y sample (XVUSY) are much more clearly observed in the 3D reconstruction obtained by electron tomography. By studying subsequent slices from the reconstruction one can obtain intricate details of the size, shape and connectivity of mesopores. Please note that the pores in XVUSY (Figure 3) are random with respect to position and vary broadly with respect to size (4 – 34 nm). Electron tomography is suited to deal with this type of nonuniform sample, where unique individual particles need to be imaged.

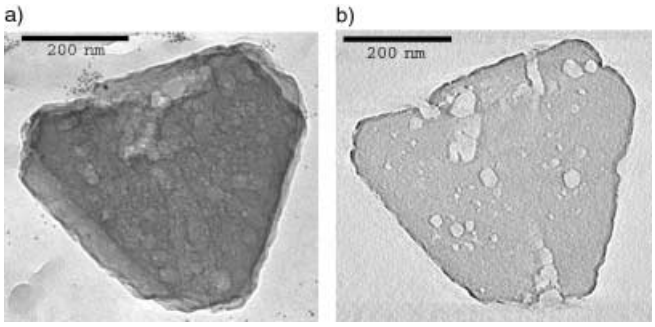

Figure 3. *a) 2D-TEM image of an XVUSY crystal and b) a thin slice (1.25 nm) through the 3D-TEM reconstruction of this crystal. Scale bars 200 nm.*

Electron Crystallography

Electron crystallography is an approach of electron microscopy where a 3D image is synthesised from a set of 2D images. A principal difference with electron tomography is that typically *two to four images* are taken of *similar, but not identical pieces* of material on a microscope grid. Thin crystals (<30 nm) are too small to be analyzed by X-ray single-crystal diffraction but are appropriate specimens for electron crystallography as electrons interact more strongly with matter than X-rays. The goal of electron crystallography is to build up the 3D Fourier transform of a repeating element by recording 2D images from crystals tilted at various angles (see Figure 2). The 2D Fourier transform of each 2D image provides a central plane through the 3D Fourier space. As such, the 2D Fourier transform provides phases as well as amplitudes. For well-ordered crystals, the resolution as provided by the 2D Fourier transforms can significantly be extended by incorporating electron diffraction patterns of the same area. The electron diffraction patterns yield amplitudes that are superior to those derived from the 2D Fourier transformed images, since the electron diffraction pattern is not influenced by the resolution-damping effect of the contrast transfer function of the microscope. In any case, when all available 2D images have been integrated into a composite 3D Fourier transform, the 3D reconstruction of the structure of interest is obtained by inverse Fourier transformation. This approach, electron crystallography, was pioneered as a 3D imaging technique within the life sciences to investigate on bacteriorhodopsin, a protein that forms ordered crystals in the membrane of a bacterium.[24]

The strength of electron crystallography as applied to structures within the field of materials sciences is impressively illustrated by the groups of Terasaki, Stucky and Ryoo. They joined forces in applying electron crystallography to determine the pore structure of ordered mesoporous materials, in particular MCM-48[25, 26] and SBA-6.[27] High-resolution transmission electron microscopy (HRTEM) images of several orientations of thin parts (<30 nm) of a specimen were collected. The different orientations have to be found in *different* parts of the sample on the grid, calling upon a high degree of homogeneity of the sample. From these images and their Fourier transforms (Figure 4) phase and amplitude information of the structure factors can be obtained. Using this information, Sakamoto et al.[27] have obtained a three-dimensional model of the pore structure of SBA-6. The results displayed in Figure 5 contain an impressively detailed picture of the bimodal pore structure that involves two types of cages (sizes 7.3 and 8.5 nm) that are interconnected by 2 nm micropores. Electron crystallography provides details on asymmetric pore size and configuration that cannot be obtained by other techniques.

Z-Contrast Tomography

Another approach of 3D imaging with electron microscopy has recently developed by Midgley and co-workers,[28, 29]

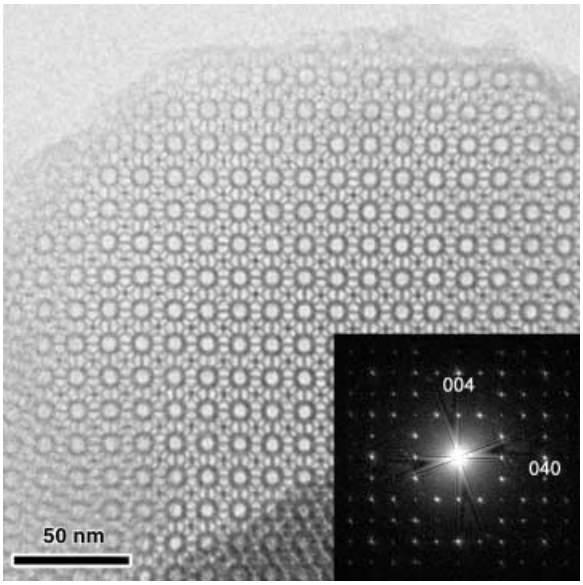

Figure 4. *An example of an HRTEM image of SBA-6 and (inset) the corresponding Fourier diffractogram; [100] orientation. Typically two to four of these data sets are needed to be able to calculate the structure.*

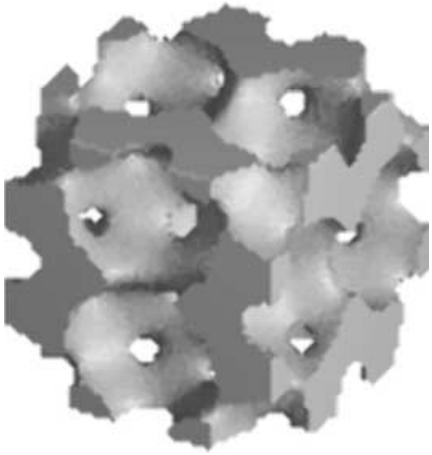

Figure 5. *Image of the 3D structure of SBA-6 obtained from data as shown in Figure 4. The structure of SBA-6 obtained from a so-called electrostatic potential map shows large A-cages and smaller B-cages with interconnecting pores.*

where images are collected—analogously to electron tomography—with the electron microscope working in the scanning (S) mode (high-angle annular dark field (HAADF) mode[12]) and not in the transmission mode (TEM). With this technique, often referred to as *Z*-contrast tomography, use is made of Rutherford scattering (*Z*-contrast) to enhance the contrast difference between light and heavy elements (the HAADF-STEM signal is approximately proportional to the square of the atomic number). As a result, this technique is suitable to image small metal particles in mesoporous silica. Furthermore, note that HAADF-STEM imaging is less sensitive to strong electron diffraction effects that prohibit the application of TEM tomography to highly diffracting samples. In Figure 6 we show the reconstructed images of palladium-ruthenium on mesoporous silica obtained from the tilt series as described above. A resolution of $\sim$1 nm has been obtained illustrated by a single bimetallic particle visible in the bottom left image.

A critical comparison between the different modes of 3D-TEM is beyond the scope of this Highlight. Sample and microscope requirements, risks of sample damage in the electron beam, complexity of data handling and image reconstruction algorithms are among the main factors to be considered. We refer to the list of references for detailed discussions of these and other issues. The main discrimination between the application of electron crystallography and tomography is in the homogeneity of the sample. In case of uniform mesopores, electron crystallography seems to be the preferred technique, whereas electron tomography can be applied to samples with nonuniform mesopores. Furthermore, for mesoporous materials electron crystallography will provide details at the microscopic scale (1 – 5 nm) whilst electron tomography provides full details at the mesoscopic scale (2 – 100 nm).

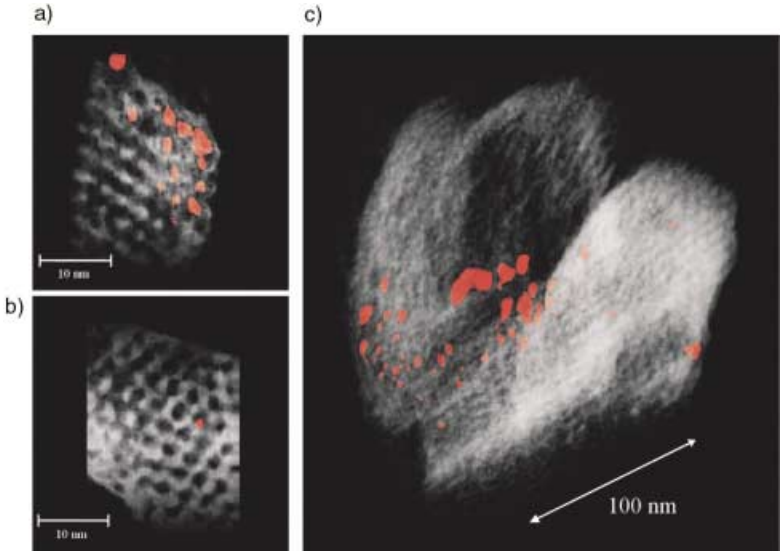

Figure 6. *Reconstructed images from a tilt series of Pd-Ru particles (red) on ordered mesoporous SiO_2. a, b) Small areas of the specimen at large magnification (scale bars 10 nm); c) an overview of the reconstructed image.*

In sum, over the last year we have noted an outburst of development and application to utilise TEM for the full 3D imaging of mesoporous materials. These strides towards 3D imaging will be of great importance to assemble catalysts, adsorbents and sensors based on this important class of materials.

Supported by NWO/CW, grant 98037. The research of A.J.K. has been made possible by support of the Royal Netherlands Academy of Arts and Sciences (KNAW). We thank Ries Janssen, Dennis Lensveld and Sandra Kemp for their valuable input.

[1] J. S. Beck, J. C. Vartuli, W. J. Roth, M. E. Leonowicz, C. T. Kresge, K. D. Schmitt, C. T.-W. Chu, D. H. Olson, E. W. Sheppard, S. B. McCullen, J. B. Higgins, J. L. Schlenker, *J. Am. Chem. Soc.* **1992**, *114*, 10834 – 10843.
[2] D. Zhao. Q. Huo, J. Feng, B. F. Chmelka, G. D. Stucky, *J. Am. Chem. Soc.* **1998**, *120*, 6024 – 6036.
[3] P. T. Tanev, T. J. Pinnevaia in *Access in Nanoporous Materials* (Eds.: T. J. Pinnevaia, M. F. Thorpe) Plenum Press, New York, NY, pp. 13 – 27.
[4] U. Ciesla, F. Schüth, *Microporous Mesoporous Mater.* **1999**, *27*, 131 – 149.
[5] G. Øye, J. Sjöblom, M. Stöcker, *Adv. Colloid Interface Sci.* **2001**, *89 – 90*, 439 – 466.
[6] a) C. Choi-Feng, J. B. Hall, B. J. Huggins, R. A. Beyerlein, *J. Catal.* **1993**, *140*, 395 – 405; b) G. R. Meima, *Cattech* **1998**, *2*, 5 – 12; c) M. Tromp, J. A. van Bokhoven, M. T. Garriga Oostenbrink, J. H. Bitter, K. P. de Jong, D. C. Koningsberger, *J. Catal.* **2000**, *190*, 209 – 214.
[7] a) J. R. Anderson, *Structure of Metallic Catalysts*, Academic Press, London, **1992**; b) K. P. de Jong, *Curr. Opin. Solid State Mater. Sci.* **1999**, *4*, 55 – 62.
[8] M. Kruk, M. Jaroniec, *J. Phys. Chem. B* **2002**, *106*, 4732 – 4739.
[9] P. I. Ravikovitch, A. V. Neimark, *Langmuir* **2002**, *18*, 1550 – 1560.
[10] J. M. Thomas, *Angew. Chem.* **1999**, *111*, 3800 – 3843; *Angew. Chem. Int. Ed.* **1999**, *38*, 3588 – 3628.
[11] J. M. Thomas, O. Terasaki, P. L. Gai, L. Pratibha, W. Zhou, J. Gonzalez-Calbet, *Acc. Chem. Res.* **2001**, *34*, 583 – 594.
[12] L. Reimer, *Transmission Electron Microscopy, Springer Series in Optical Sciences, Vol. 36* (Ed.: P. W. Hawkes), Springer-Verlag, Berlin, **1997**.
[13] W. Coene, G. Janssen, D. Van Dyck, M. Op de Beeck. *Phys. Rev. Lett.* **1992**, *69*, 3743 – 3746.
[14] A. Orchowski, W.-D. Rau, H. Lichte, *Phys. Rev. Lett.* **1995**, *74*, 399 – 402.
[15] A. Datye, *Top. Catal.* **2000**, *13*, 131 – 138.
[16] A. J. Koster, U. Ziese, A. J. Verkleij, A. H. Janssen, K. P. de Jong, *J. Phys. Chem. B* **2000**, *104*, 9368 – 9370.
[17] W. Baumeister, R. Grimm, J. Walz, *Trends Cell Biol.* **1999**, *9*, 81 – 55.

[18] B. F. McEwen, M. Marko, *J. Histochem. Cytochem.* **2001**, *49*, 553 – 564.
[19] *Electron Tomography* (Ed.: J. Frank) Plenum Press, New York, NY, **1992**.
[20] A. J. Koster, R. Grimm, D.Typke, R. Hegerl, A. Stoschek, J. Walz, W. Baumeister, *J. Struct Biol.* **1997**, *120*, 276 – 308.
[21] U. Ziese, A. H. Janssen, J. L. Murk, W. J. C Geerts, T. Krift, A. J. Verkleij, A. J. Koster, *J. Microscopy* **2002**, *205*, 187 – 200.
[22] W. Baumeister, A. C. Steven, *Trends Biochem. Sci.* **2000**, *25*, 624 – 631.
[23] A. H. Janssen, A. J. Koster, K. P. de Jong, *Angew. Chem.* **2001**, *113*, 1136 – 1138; *Angew. Chem. Int. Ed.* **2001**, *40*, 1102 – 1104.
[24] R. Henderson, P. N. Unwin, *Nature* **1975**, *257*, 28 – 32.
[25] A. Carlsson, M. Kaneda, Y. Sakamoto, O. Terasaki, R, Ryoo, S. H. Joo, *J. Electron Microsc.* **1999**, *48*, 795 – 798.
[26] M. Kaneda, T. Tsubakiyama, A. Carlsson, Y. Sakamoto, T. Ohsuna, T. Terasaki, S. H. Joo, R. Ryoo, *J. Phys. Chem. B* **2000**, *106*, 1256 – 1266.
[27] Y. Sakamoto, M. Kaneda, O. Terasaki, D. Y. Zhao, J. M. Kim, G. D. Stucky, H. J. Shin, R. Ryoo, *Nature* **2000**, *408*, 449 – 453.
[28] P. A. Midgley, M. Weyland, J. M. Thomas, B. F. G. Johnson, *Chem. Commun.* **2001**, 907 – 908.
[29] M. Weyland, P. A. Midgley, J. M. Thomas, *J. Phys. Chem. B* **2001**, *105*, 7882 – 7886.

Received: May 24, 2002 [H 427]